Development of a Guidance and Control Design Tool for Entry Space Vehicles with different Lift-over-Drag Ratios

Luís Guerreiro
MSc in Aerospace Engineering
Instituto Superior Técnico, Universidade Técnica de Lisboa
Avenida Rovisco Pais, 1-1049-001 Lisboa, Portugal

July 20, 2011

Abstract

A re-entry simulation tool - REACTIVE - that allows for the analysis and design of different guidance and control tecniques was developed. It integrates a 3-DoF simulator and several guidance algorithms, namely the Apollo Entry Guidance, the Shuttle Entry Guidance and the Enhanced E-Guide, a guidance scheme for a high lift-over-drag vehicle that uses the Non-linear Dynamic Inversion technique.

A semi-analytical procedure for the generation of a longitudinal profile tailored for the targeting phase (triggered at $V \approx 5$ km/s and lasting up to Terminal Area Energy Management conditions) of a high lift-over-drag re-entry vehicle was also developed and integrated in REACTIVE. The procedure, validated through a series of Monte-Carlo tests, generates a reference profile using analytical approximations of the altitude and flight-path angle which ensure that initial and final conditions are met, while the downrange criteria is satisfied by means of Least-Squares and determination of the suitable bank angle law. This semi-analytical approach allows instantaneous generation of the reference profile and is thus suitable for onboard installation.

The REACTIVE tool collects all these guidance and control approaches in the same simulation environment, and successfully generalizes them, so that they are not restricted to the associated baseline vehicles and are suitable to be applied to the respective vehicle classes, which range from capsules to moderate and high lift-over-drag vehicles. Having been used for Earth re-entry, REACTIVE has also been extended to the Mars scenario.

Keywords: re-entry, guidance and control, entry space vehicles, lift-over-drag, simulation tool, Apollo, Space Shuttle, high lift, reference profile generation, TAEM targeting.

1 Introduction

Atmospheric entry is one of the most intricate problems in the Aerospace domain. It concerns the dynamics and kinematics of a body coming from space that encounters significant planet atmosphere along its trajectory, either descending from a planet orbit, or originating from eccentric hyperbolic orbits. Three outcomes are possible once atmospheric contact is established: the body may skip out of the atmosphere and return to space; the body may be destroyed due to the action of atmospheric resistance; the body may traverse through the atmospheric layer and reach the planet surface.

This last case is possible only if the angle with which it impacts the atmospheric layer is within a tight range of values, or in other words, if the Entry Interface Point (EIP) conditions are within the interval that leads to feasible re-entry trajectories, denominated entry corridor. This scenario may be divided in three different types of entry configurations: ballistic entry, lifting entry, and skip entry (which has never been used). The categorization of an entry configuration is determined by the ability of the vehicle to generate a lift force when entering the planet atmosphere - its lift-to-drag ratio (L/D) characteristics.

Approximate ballistic entry occurs when the body's L/D is low, tipically when $L/D < 0.5$, which is the case of intercontinental missiles, or capsule-like vehicles, *e.g.* the Apollo Command Module (Apollo CM) or the Soyuz. In a ballistic entry the body follows

an almost straight path through atmosphere, sustaining high heat fluxes and significant g-loads. Its point of impact is almost fully determined by its entry angle in the atmosphere, and reduced steering is available (or no steering at all, if $L/D = 0$).

In the case of lifting entry it is considered that $L/D \geq 0.5$. The only example that exists of successful lifting entry is the Space Shuttle Orbiter, that uses its ability of generating a significant lift force to dissipate energy in a controlled fashion during re-entry, being also capable of changing its trajectory to reach the landing site safely. While in a ballistic setting the entry body becomes invariably wasted, in lifting entry it is possible to reuse the re-entry body.

In order to deal with the complex issue of dissipating these amounts of energy, the banking capabilities of the entry body can be used, in the case where $L/D > 0$. This consists in laterally rotating the vehicle from the local vertical (defined as the direction of the gravity force), *i.e.* banking the vehicle, hence re-directing the lift vector, reducing its vertical component and increasing its lateral component. With reduced lift in the vertical direction, the descent rate and the aerodynamic decelaration increase, which is equivalent to breaking the RV longitudinally.

In the case of a re-entry vehicle (RV), the banking maneuvers are selected by a Guidance and Control (GC) system, that is responsible for guiding and controlling the RV through its entry trajectory until the Terminal Area Management (TAEM) conditions are met, mitigating the effects of uncertainties. The guidance function uses the estimates provided by navigation to produce reference commands, while the control function is responsible for tracking this reference.

Several guidance and control methods are available, as identified in [16]. Generally, a distinction between predictor based guidance schemes and reference trajectory tracking guidance schemes is made and, under these two groups, several entry guidance methods are identified and discussed. Generally, predictor based guidance schemes suffer from being computationally demanding, which is a barrier to its on-board implementation. On the other hand, the bulk of the computation of the reference trajectory tracking algorithms is done off-line, which reduces the required computational loads, but profile adaptability is lost. The most successful entry algorithms are based on a reference profile generated off-line and stored on-board, which is tracked with gain-scheduled Proportional-Integral-Derivative (PID) controllers [15]. Notable examples of this are the Apollo [1], the Shuttle [5] and the Soyuz [6] Entry Guidance schemes.

Recently, guidance solutions with increased flexibility in reference profile generation and adaptable to uncertainties have been developed. In [3], a scheduled gains Linear Quadratic Regulator (LQR) controller is used to track a reference profile using energy as the independent variable. It is proved that the same controller gains can be used for different reference trajectories, provided that the RV is the same. In [10] the Shuttle Entry configuration is used as baseline for the development of an on-board reference trajectory generation algorithm, and a controller based on [3] is used to track the generated reference profile. In [2] an innovative re-entry algorithm developped for a high lift-over-drag RV is presented, where the guidance solution consists of two different methods, feedback linearization through Non-linear Dynamic Inversion technique, and tracking via LQR control of a reference profile generated on-board.

In this work, a re-entry guidance and control design tool, named REACTIVE, that integrates the Apollo Entry Guidance [1] (developed by NASA and prototyped by GMV), the Enhanced E-Guide [2] (developed and prototyped by GMV), and the Shuttle Entry Guidance scheme, which was developed by NASA and prototyped for the tool, is implemented. The core of the tool uses a point-mass three degree of freedom (3-DoF) simulation setting implemented in MATLAB, that allows for the addition of different RVs and guidance schemes.

A semi-analytical procedure for on-board profile generation that enables precise landing site targeting for high L/D RVs was also developed, tested, and added to the tool. The reason for its development was the mediocre performances of the on-board reference profile generation algorithm implemented in Enhanced E-Guide in the landing site targeting phase, namely its excessive computation times due to the use of the shooting method [12], which would certainly be a barrier to its on-line implementation. In that respect, the newly developed solution is computationally lighter and more accurate with respect to the downrange requirement. The procedure generates a reference profile semi-analytically by pre-estimating profiles for altitude and flight-path angle, directly evaluating of the equations of motion, and determines the downrange profile by analytical integration of the downrange equation using the linear least squares method [14]. The associated bank angle law is computed so that the downrange requirement is precisely met. This profile generation algorithm was tested using PID control for the reference tracking, and it was further validated through Monte-Carlo tests.

REACTIVE thus collects all these guidance schemes and integrates them in one single tool. The associated baseline vehicles, the Apollo CM, the Shuttle Orbiter, and the Plane-shaped Hypersonic Orbital Entry BUS (Phoebus) concept vehicle were also

added to REACTIVE's RV database. Furthermore, REACTIVE aims at extending the available guidance schemes to the associated RV L/D class. This means that the prototypations of the guidance schemes, which were tested and validated using the associated baseline vehicles, were generalized and made independent of their baseline vehicles, so that each of the algorithms was made addaptable to different RVs. Therefore, the Apollo Entry Guidance is now suitable for the broader capsule-like RV class, the Shuttle Entry Guidance is suitable for the moderate L/D RV class, and the Enhanced E-Guide is suitable for the high L/D class. Finally, the planet Mars environment, for which there are a number of projects under way promoted by ESA and NASA, was added to REACTIVE.

2 Simulation

2.1 Equations of motion

The equations of motion, written in the reference frame which has one axis aligned with the RV velocity vector (relative to the planet), the other axis aligned with the vector orthogonal to the plane formed by the RV position and velocity vectors, and the third axis such that the reference is right-handed, are [8, 10]

$$\frac{\mathrm{d}\,h}{\mathrm{d}\,t} = V\sin\gamma, \tag{1a}$$
$$\frac{\mathrm{d}\,\chi}{\mathrm{d}\,t} = V\frac{\cos\gamma\sin\psi}{r\cos\lambda}, \tag{1b}$$
$$\frac{\mathrm{d}\,\lambda}{\mathrm{d}\,t} = V\frac{\cos\gamma\cos\psi}{r}, \tag{1c}$$
$$\frac{\mathrm{d}\,V}{\mathrm{d}\,t} = -D - g\sin\gamma + \omega^2 r\cos\lambda\left[\sin\gamma\cos\lambda - \sin\lambda\cos\gamma\cos\psi\right], \tag{1d}$$
$$\frac{\mathrm{d}\,\gamma}{\mathrm{d}\,t} = \frac{1}{V}\left[\left(\frac{V^2}{r} - g\right)\cos\gamma + L\cos\sigma + 2\omega V\cos\lambda\sin\psi + \omega^2 r\cos\lambda\left(\cos\gamma\cos\lambda - \sin\gamma\sin\lambda\cos\psi\right)\right], \tag{1e}$$
$$\frac{\mathrm{d}\,\psi}{\mathrm{d}\,t} = \frac{1}{V}\left[L\frac{\sin\sigma}{\cos\gamma} + \frac{V^2}{r}\cos\gamma\sin\psi\tan\lambda - 2\omega V\left(\tan\gamma\cos\lambda\cos\psi - \sin\lambda\right) + \frac{\omega^2 r}{\cos\gamma}\sin\lambda\cos\lambda\sin\psi\right], \tag{1f}$$

where r is the RV distance to the Earth center, h is the altitude ($r = R + h$, where R is the Earth radius), χ is the latitude and λ the longitude, V is the RV velocity norm, γ is the flight path angle (FPA), and ψ is the heading angle, defined as the angle measured from North in the clockwise direction. Moreover, L and D are the aerodynamic lift and drag force norms per unit mass, g is the norm of the gravity vector, and σ is the bank angle. Equations (1)[1] are propagated to simulate the re-entry motion of the RV.

2.2 Boundaries and constraints

The re-entry problem is bounded by the EIP and TAEM conditions, and also by the entry corridor constraints. For 3-DoF re-entry analysis, the maximum heat flux, aerodynamic acceleration, and dynamic pressure, and the equilibrium glide condition, all mappable in the altitude-velocity plane, are the most relevant path constraints:

$$\dot{Q} \leq \dot{Q}_{\max}, \tag{2a}$$
$$\left\|\vec{L} + \vec{D}\right\|/g_n \leq n_{\max}, \tag{2b}$$
$$q \leq q_{\max}, \tag{2c}$$
$$\left(\frac{V^2}{r} - g\right)\cos\gamma + L\cos\sigma \leq 0, \tag{2d}$$

where $g_n = 9.80665\ m/s^2$ is the standard gravity, n is an integer referring to number of g's. Equation (2a) represents the constraint in maximum heat flux, where heat flux $\dot{Q}$ is written as $\dot{Q} = C\rho^{\frac{1}{2}}V^{3.15}$, with C a multiplying constant[2]. Equation (2b)

[1] In fact, in the simulator these equations are written and propagated in the ECEF reference frame.

[2] This expression for heat flux is an approximate expression for convective and radiative heating at stagnation point for a body entering the Earth atmosphere [4, 13]

is the maximum g-load constraint that depends on the vehicle structure or on the presence of human beings on-board. Equation (2c), where $q = \frac{1}{2}\rho V^2$, expresses the constraint on dynamic pressure. Finally, equation (2d) is the equilibrium glide condition. This last condition is not a hard constraint, in the sense that it serves to reduce the phugoid oscillations, being more meaningfull at higher altitudes.

2.3 Atmospheric, aerodynamic and planet environment models

Different databases are used for evaluation of (1). The atmospheric database is a mapping of air density ρ, air temperature, air pressure, and sound speed v_s with respect to altitude h. The RV aerodynamic database contains all the information related to the RV, including the lift $C_L(\alpha, M)$ and drag $C_D(\alpha, M)$ coefficients mapped with respect to the angle of attack α and the Mach number M. The planet environment database contains all the planet related parameters, being the more important the gravitational parameter μ, the planet angular velocity ω, and the planet radius R.

3 Guidance schemes

3.1 Generalization of the Shuttle Entry Guidance

The Shuttle Entry Guidance [5] uses a reference profile computed offline and stored on-board, based on analytical expressions with arbitrary coefficients that relate velocity (or energy) with drag, which is tracked via a gain-scheduled PID controller. The generalization of this algorithm consisted on the addition of two functionalities in REACTIVE: the arbitrary definition of the drag-velocity profile and the analytic computation of the scheduled gains, so as to make this algorithm adaptable and reconfigurable to different RVs.

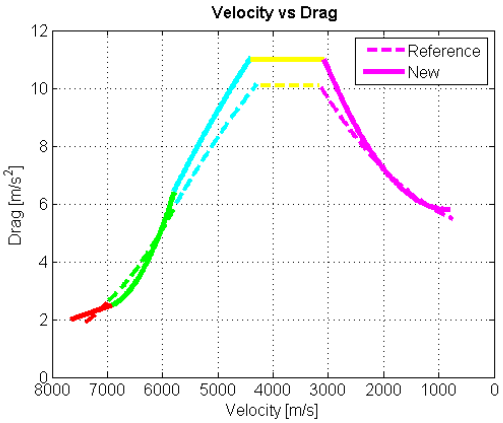

Figure 1: Reference profile for moderate L/D RV and newly constructed profile.

Flexibility in the design of the entry profile is achieved In REACTIVE by setting the drag relations coefficients at will, as shown in figure 1, while the analytical drag-velocity expressions for each phase are retained, as are all the other expressions derived thereof.

Regarding the gain computation, the analytical relations for gains f_1 and f_2 derived in [5] are used. For their evaluation it is required a detailed knowledge of the aerodynamic database, namely of the derivative of the drag coefficient. In [5] it is suggested that C_{D_0} $\dot{C}_{D_0}$ are approximated by a second order polynomial to model the C_D dependence on the angle of attack α, and an exponential relation to model the C_D dependence on the Mach number. However, in order to make this implementation more flexible, the approximation of C_D used in REACTIVE uses a combination of two polynomial expressions of arbitrary order, one dependent on the angle of attack and the other of the Mach number:

$$C_D = \mathrm{K}_{0_\alpha} + \mathrm{K}_{1_\alpha}\alpha + \cdots + \mathrm{K}_{n_\alpha}\alpha^{n_\alpha} + \mathrm{K}_{0_M} + \mathrm{K}_{1_M}M + \cdots + \mathrm{K}_{n_M}M^{n_M} \tag{3a}$$

$$\dot{C}_D = \dot{\alpha}\left(\mathrm{K}_{1_\alpha} + 2\mathrm{K}_{2_\alpha}\alpha + \cdots + n\mathrm{K}_{n_\alpha}\alpha^{n_\alpha - 1}\right) + \dot{M}\left(\mathrm{K}_{1_M} + 2\mathrm{K}_{2_M}M + \cdots + n\mathrm{K}_{n_M}M^{n_M - 1}\right), \tag{3b}$$

where n_α and n_M are the arbitrary order of the polynomial. Equation 3b enables the evaluation of $\dot{C}_D$ for any RV.

3.2 Apollo derivatives computation

The Apollo Entry Guidance consists of two main phases: the atmospheric capture, where the capsule is rotated so as to have its lift vector directed downwards, and the targeting phase, where a reference profile is tracked using a scheduled-gains PID controller. In order to make this algorithm suitable for any capsule-like vehicle, and assuming that a reference trajectory associated to the RV is available, it is necessary to compute the scheduled gains in a systematic manner.

The gains F_1 (the derivative of range with respect to atmospheric drag), F_2 (the derivative of range with respect to vertical velocity), and F_3 (the derivative of range with respect to the L/D) are the derivatives of range with respect to the control variables. In REACTIVE they are analytically computed, using (1) and the approximations suggested in the Appendix of [1]. The expressions found are:

$$F_1 = \frac{V^2 \cos\gamma}{V\frac{\dot{h}}{H_s} + 2\left(-D - g\sin\gamma\right)} \frac{1}{D} \frac{\mathrm{ATK}}{R}, \tag{4a}$$

$$F_2 = \frac{V\cos\gamma}{\left(\frac{V^2}{r} - g\right)\cos\gamma + D\frac{L}{D}} \frac{\mathrm{ATK}}{R}, \tag{4b}$$

$$F_3 = \frac{s_{\mathrm{ref}}}{L/D}, \tag{4c}$$

where ATK/R is a multiplying constant. Expressions (4) are evaluated using the reference trajectory values in figure 16 of [1], and compared against the reference results in figure 2.

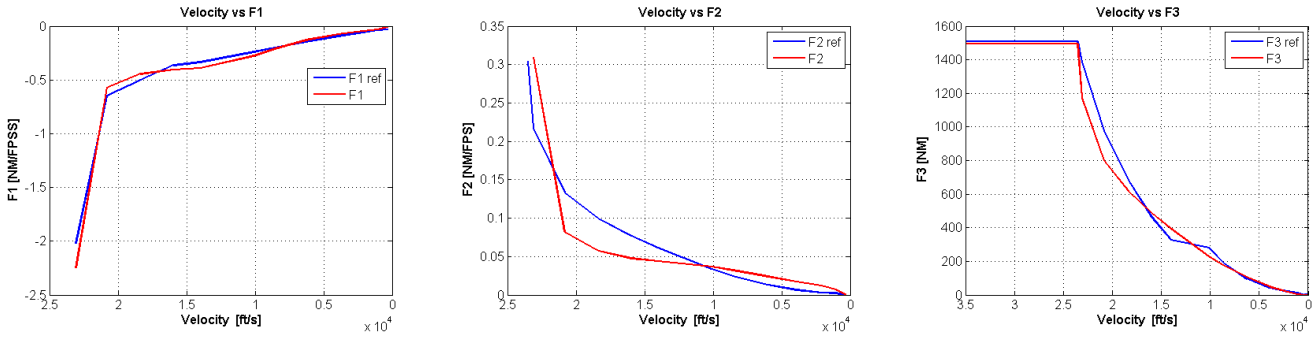

(a) F_1 derivative comparison; (b) F_2 derivative comparison; (c) F_3 derivative comparison;

Figure 2: Tabled derivatives in blue against analytically computed derivatives in red.

The tabled numerical derivatives F_1 and F_3 are closely matched by the derived analytical results, while F_2 is slightly mis-approximated. This difference may be a consequence of mismatches in the atmospheric model and in the RV aerodynamic model. However, implementation of the analytically computed gains in REACTIVE provide satisfactory results.

3.3 Flexibilization of Enhanced E-Guide

Enhanced E-Guide uses feedback linearization through Non-linear Dynamic Inversion (NDI) control [17] in the first entry phases, and a Linear Quadratic Regulator (LQR) gain-scheduled controller [3] for reference trajectory tracking in the last phase of landing site targeting. This makes the algorithm adaptable to different RVs, as the computation of the guidance law takes directly into account the RV dynamics. Therefore, the only changes made to Enhanced E-Guide were related with the NDI phases: the threshold for phase change and the altitude and heat flux references (which are tracked by the NDI controller) were made user-definable parameters (3).

In this way, the Enhanced E-Guide can be tailored to different high L/D vehicles. Note that it is possible to omit one of the phases, if desired, or interchange its order. Ultimately, REACTIVE's generalization of Enhanced E-Guide can be seen as an

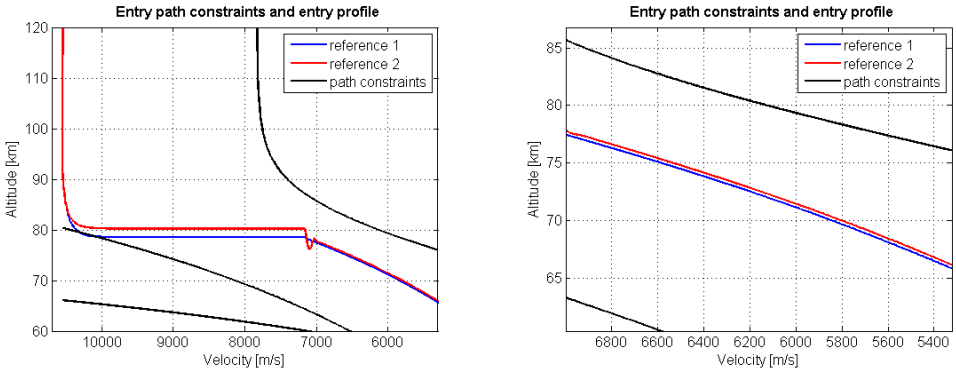

(a) Altitude and heat flux references tracking; (b) Detail of heat flux tracking;

Figure 3: High L/D RV on Enhanced E-Guide, following two different altitude and heat flux references.

implementation of three independent guidance schemes - altitude tracking with NDI, heat flux tracking with NDI, and tracking of onboard-generated reference profile - which can be selected and concatenated at will.

4 Guidance for landing site targeting

Two approaches for solving the boundary value problem of a high L/D RV targeting phase were followed. Both seek a bank angle law dependent on the velocity $\sigma(V)$ that meets initial and final conditions, and the range requirements. To verify compliance with this last requirement, the downrange equation [4]

$$\frac{\mathrm{d}s}{\mathrm{d}V} = -\frac{R}{R+h}\frac{V\cos\gamma}{-D-g\sin\gamma} \tag{5}$$

must be integrated. In the derivations, only longitudinal motion given by (1a), (1d), (1e) is considered[3].

4.1 Approximate analytic solution

In the analytic approach, it is assumed that FPA is constant and zero throughout the targetting phase, the distance to center of planet $r = R + h$ is constant, the L/D is constant, and the bank angle σ is constant. This allows to find a relation between the downrange, velocity and bank angle, based on (5), and integrate it analytically with respect to V:

$$\cos\sigma = \frac{(s-s_0)}{\frac{R_E}{2}\cos\gamma\frac{C_L}{C_D}}\log\left[\frac{V^2+gr}{V_0^2+gr}\right]^{-1}, \tag{6}$$

which is a closed analytical relation between the bank angle, the downrange requirement, and velocity.

However, the simplifications made assume implicitly a profile for FPA (constant and zero) and altitude (constant), which is not true when the landing site is approached. Furthermore, the L/D is not constant either, varying in the $[2.0,\ 2.5]$ interval, and is another source of error. This mismodeling thus results in a loss of accuracy in the solution in terms of downrange, even though the final downrange constraint is strictly imposed.

4.2 Reference profile generation procedure

4.2.1 Procedure description

The simplified analytical solution obtained in section 4.1 has shortcomings intrinsically related with the approximations performed on the set of differential equations that model the system dynamics. In the Reference Profile Generation (RPG) procedure, instead of simplifying (5) to enable integration, this expression is approximated by a polynomial dependent on the velocity V, which is

[3]Lateral motion decoupling is achieved by neglecting atmosphere rotational effects ($\omega = 0$ in (1)) which are low compared to other forces.

Table 1: Configuration used for the Monte-Carlo shots

State	Nominal initial conditions	Standard deviation	Units
λ	2.5	0.05	deg
ϕ	-93.3	2.5	deg
h	65183	30	m
V	5270	5	m/s
γ	-0.1832	0.001	deg
ψ	84.9851	0	deg

then integrated with respect to V to obtain $s(V)$. This approximation is performed using the least squares technique [14], which requires the evaluation of (5). For this evaluation, approximate altitude and FPA profiles, and a bank angle law, are necessary. Therefore, the RPG procedure initially selects a bank angle law, subsequently determines the altitude and FPA profiles, and finally the evaluates (5), approximates it using least squares [14], and analytically integrates the polynomial obtained.

In this process, the bank angle law is selected prior to downrange evaluation. However, the central problem is to find a bank angle that satisfies the downrange requirement, and not a bank angle law that imposes a downrange. Therefore, this process is used to determine a mapping $\sigma(s_{\mathrm{t}})$ between the bank angle σ and the total downrange s_{t}, by repeating it a pre-defined number of times, *e.g.* 10 or 20 (depending on the desired accuracy), for different bank angle laws. Once the mapping is found, the bank angle is determined by evaluating $\sigma(s_{\mathrm{t}})$ for the desired total downrange, $s_{\mathrm{t_D}}$.

Since the initial and final boundary conditions and the downrange requirement must be verified, the bank angle law, defined as being dependent on velocity, must have three free parameters: two are used to ensure that the bank angle law satisfies the initial and final boundary conditions, and the third parameter is selected so that the downrange requirement is met.

The determination of the altitude h and FPA γ profiles is made in two steps: the estimation of the state-variables appearing in (1a), (1d), (1e), and the direct evaluation of the equations of motion by using the estimated variables. In the estimation of the state-variables it is assumed that (1a), (1d), (1e) are dependent on velocity only, while the remaining variables appearing on the expressions are considered to be parameters dependent on velocity, that must also be estimated. This is an important assumption that reduces the complexity of the problem, as the equations are 'integrated' and become decoupled. Furthermore, the boundary conditions are strictly enforced in the estimation step using a simple implementation of the collocation method [18]. This ensures that when the equations of motion are evaluated by substitution of the estimated parameters, initial and final boundary conditions are exactly satisfied.

4.2.2 Testing

For testing the targeting ability of the algorithm, a Monte-Carlo test was performed using the uncertainties in initial conditions as presented in table 1. Furthermore, an uncertainty of 20% in the air density and of 10% in the RV aerodynamic database were also considered. The Monte-Carlo test consisted of 1000 shots with the uncertainty set described above, for a 3-sigma (99.7%) success probability with a 95% confidence interval. The results of the tests are depicted in figure 4.

The results show that the RPG enables a good targeting precision. In the histogram in 4b, it is seen that the final downrange dispersion amounts to a 10 km interval around the desired target. The bias of 2 km shown in the histogram could further be corrected once the lateral motion is accounted for, which would additionally reduce the width of the 10 km interval.

5 The REACTIVE tool

REACTIVE integrates the generalized Shuttle Entry Guidance, Apollo Entry Guidance, and Enhanced E-Guide algorithms, and the newly developed RPG procedure, being shaped to run all the vehicles and guidance schemes implemented. The generalization of the guidance algorithms consisted in making the Apollo, Shuttle, and Enhanced E-Guide entry algorithms suited for low, moderate, and high lift-over-drag RV classes, respectively. Therefore, more than collecting pre-existing guidance schemes, REACTIVE recycles them so that they can be used or re-designed for the simulation of new concept vehicles.

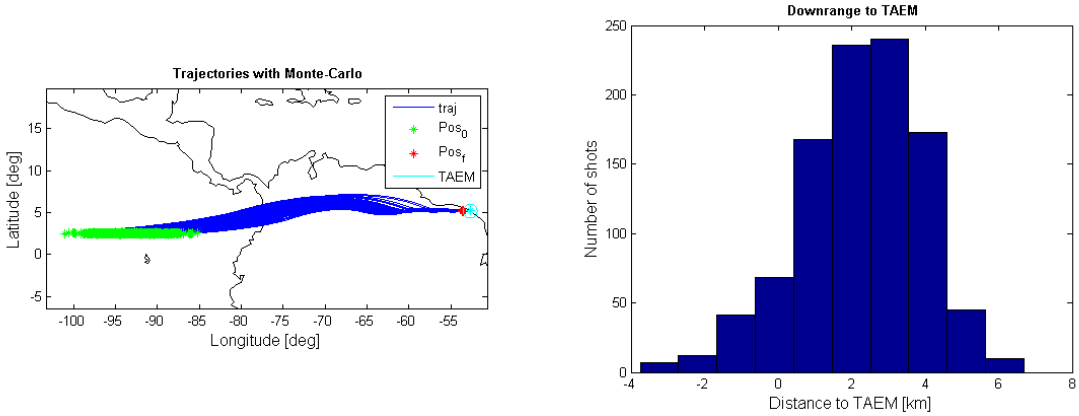

(a) Latitude-longitude trajectories; (b) Histogram of the downrange to TAEM;

Figure 4: Monte-Carlo targeting results for the RPG procedure.

5.1 L/D class study

The guidance algorithms implemented were tested for different L/D RVs belonging to the associated class, in order to explore the limits of applicability of each algorithm. The results show that the Apollo Entry Guidance is suitable for RVs in the range $0.2 < L/D < 0.6$. For lower values of L/D, the RV L/D margin is not enough to track the reference profile in the targeting phase, and is not enough to avoid violation of the constraints right after capture. This is visible in figure 5a, for the case of $L/D = 0.2$, where right after the vehicle is captured into the planet atmosphere there is barely sufficient lift available to avoid violation of the maximum heat flux constraint. For higher L/D values, the capsule begins to show an undesired oscillatory motion that may result in the violation of the constraints.

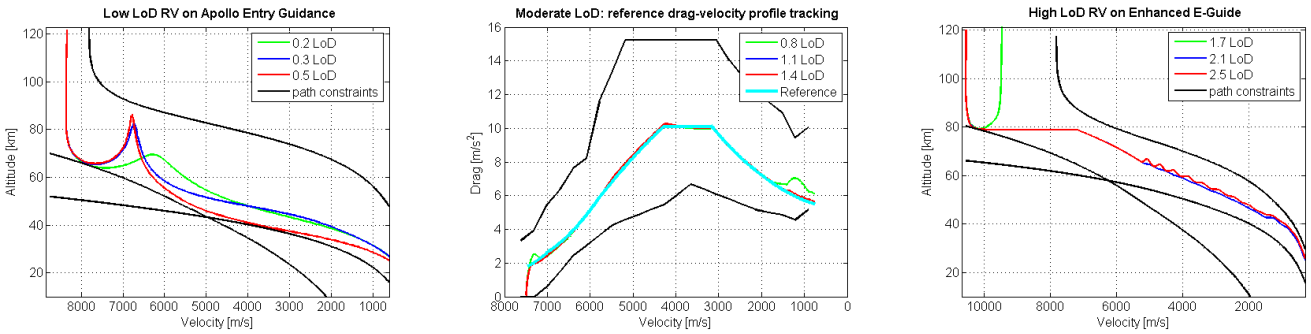

(a) Low L/D on Apollo Entry Guidance; (b) Moderate L/D on Shuttle Entry Guidance; (c) High L/D on Enhanced E-Guide;

Figure 5: Study of the RV L/D class, running on the associated guidance scheme: entry profiles and path constraints.

For the Suttle Entry Guidance, it is verified that the algorithm is suitable for $L/D > 0.8$. Below this value, the RV does not have the L/D margin to track the reference drag-velocity profile. This is further shown in figure 5b, where for the $L/D \approx 0.8$ considered the RV is not able to track satisfactorily the reference profile in the early and latest parts of re-entry. For higher L/Ds, the RVs seem to run perfectly well in the Shuttle Entry Guidance, as the higher the L/D margin, the easier it is to track the reference.

Finally, the Enhanced E-Guide is the most demanding of the three algorithms in terms of L/D requirements. It is only suitable for RVs with $1.8 < L/D < 2.5$, as the L/D margin is critical for the tracking of the reference altitude in the first NDI phase. For L/Ds below this threshold, it was verified that the RV was not able to track the reference altitude and skipped out of the atmosphere. This is further shown in figure 5c, for a RV $L/D = 1.7$. For higher L/Ds, a problem concerned with the LQR controller starts to show in the last phase. Clearly, as documented in figure 5c for the $L/D = 2.5$ case, there is an undesired oscillatory motion below $V = 5$ km/s. This results from the scheduled gains of the LQR controller not being adequate to the

new vehicle configuration.

5.2 Mixing guidance schemes and associated vehicle class

In another test, the guidance schemes and the RV class were mixed in REACTIVE. As an example of this, the Shuttle Entry Guidance is tested with the low and high L/D RVs. It is expected that the low L/D RV performs poorly in the tracking of the drag-velocity profile, while the high L/D RV shoud excel at that. The results confirm this supposition, as is shown in figure 6.

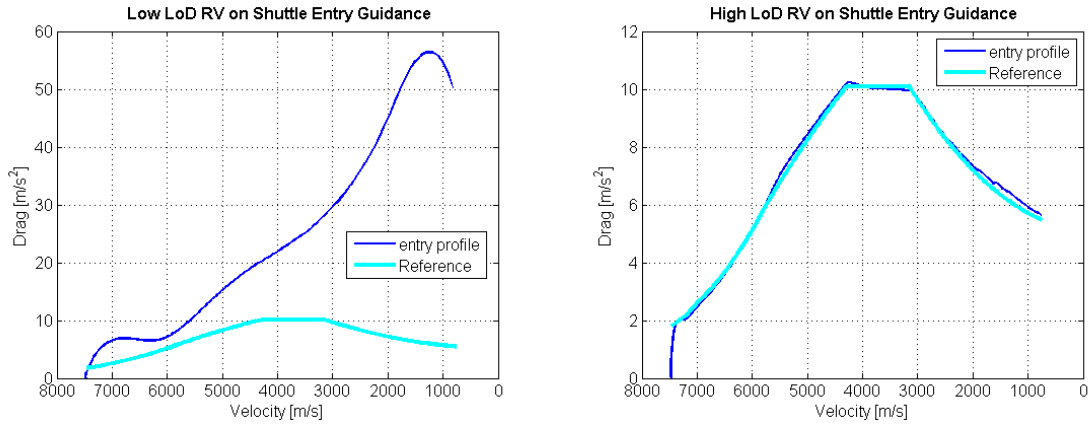

(a) Low L/D RV on the Shuttle Entry Guidance; (b) High L/D RV on the Shuttle Entry Guidance;

Figure 6: Mixing RVs and guidance schemes: low and high L/D RV on Shuttle Entry Guidance, in the drag-velocity plane.

The low L/D vehicle is not able to track the reference profile, as it has not enough L/D margin to do so. However, the approach followed in the Shuttle Entry Guidance method could in theory be applicable to low L/D RVs, provided that the reference profile was re-designed and adapted to this type of RVs. On the other hand, the high L/D RV tracks satisfactorily the drag-velocity reference profile, without requiring any modification to the profile.

5.3 Extension to Mars scenario

Mars atmosphere [11] and environment [7] have been added to REACTIVE's database. When compared to Earth, Mars gravitic acceleration is modest and its atmosphere is less dense, and relatively unknown regarding its composition. Entry strategies have thus relied on capsule-like RVs with $L/D \approx 0$. While this constrains the applicability of GC solutions to this planet scenario, it would be possible to tailor the Apollo Entry Guidance for Mars entry, provided that some minimum L/D is available [9].

6 Conclusions

In this work three entry guidance schemes, the Apollo Entry Guidance, the Shuttle Entry Guidance, and Enhanced E-Guide, were revisited. For the integration of these guidance approaches in a single simulation environment, a 3-DoF simulation setting was implemented, and the three algorithms were further consolidated and generalized. This enabled each of the guidance schemes to run on RVs belonging to the associated L/D class, instead of being restricted to the specific RVs used as baseline.

Furthermore, a semi-analytical guidance approach that solves the boundary problem of the TAEM targeting phase for an high L/D RV was developed. This procedure generates a reference profile fully compliant with the boundary conditions and constraints of the problem, as well as a bank angle law that ensures meeting the downrange requirement. These can be fed to a lower level controller for reference tracking. The results obtained under Monte-Carlo testing show that the procedure is able to cope with the uncertainties considered, due to flexible profile generation. The procedure is also deemed suitable for on-board installation, as its mostly analytical implementation allows for instantaneous entry profile generation and is not computationally demanding. It is noted that despite the tests conducted used a high L/D RV as baseline, there is no reason for this approach not to work with moderate or low L/D RVs, provided that final conditions (namely donwrange requirement) are adjusted accordingly.

Finally, REACTIVE, an entry simulation tool that allows for the design and testing of guidance and control solutions in a 3-DoF setting, was also developed. It results from the integration and consolidation of all the implemented algorithms. The tool thus comprises generalized algorithms suitable for low, moderate and high L/D RVs, which enable testing entry solutions for all RV L/D classes. The guidance schemes implemented can be freely used, and even combined, to evaluate past entry solutions, or to devise and test new entry approaches for different scenarios and RVs.

References

[1] I. Bogner. Description of Apollo Entry Guidance. Technical memorandum, NASA, 1966.

[2] E. Di Sotto, J. Branco, R. Savino, M. De Stefano Fumo, R. Monti, M. Taushe, R. Janovsky M. Scheper, J. Apeldoorn, and R. C. Molina. PHOEBUS: GNC design and performance assessment for super orbital re-entry. In *American Institute of Aeronautics and Astronautics conference*, 2009.

[3] Greg A. Dukeman. Profile-Following Entry Guidance using Linear Quadratic Regulator Theory. *American Institute of Aeronautics and Astronautics Guidance, Navigation, and Control Conference and Exhibit*, pages 5–8, 2002.

[4] Michael D. Griffin and James R. French. *Space Vehicle Design*, chapter 6 Athmospheric Entry, pages 231 – 271. Education Series. American Institute of Aeronautics and Astronautics, 2 edition, 1991.

[5] J. C. Harpold and C. A. Graves. Shuttle Entry Guidance. Technical memorandum, NASA, 1979.

[6] A. Krishnan, U. Rajeev, and R. Harikumar. Trajectory control of a winged entry vehicle to a reference drag-energy profile. In *10th National Conference on Technological Trends*, 2009.

[7] NASA. Mars fact sheet. http://nssdc.gsfc.nasa.gov/planetary/factsheet/marsfact.html. [Online; accessed 1-July-2011].

[8] Frank J. Regan and Satya M. Anandakrishnan. *Dynamics of Atmospheric Re-Entry*. Education Series. American Institute of Aeronautics and Astronautics, 1966.

[9] Jeffrey S. Robinson and Kathryn E. Wurster. Trajectory and aeroheating environment development and sensitivity analysis for capsule-shaped vehicles. *American Institute of Aeronautics and Astronautics*, 2005.

[10] Zuojun Shen and Ping Lu. Onboard generation of three-dimensional constrained entry trajectories. *Journal of Guidance, Control and Dynamics*, 26(1), 2003.

[11] SRE-PAP. Mrep mars environmental document. Sp, ESA, Keplerlaan 1, 2201 AZ Noordwijk, The Netherlands, 2010.

[12] J. Stoer and R. Bulirsh. *Introduction to Numerical Analysis*, chapter 7.3. New York Springer-Verlag, 1980.

[13] Michael E. Tauber. A review of high-speed, convective, heat-transfer computation methods. Technical Paper 2914, NASA, Ames Research Center, Moffett Field, California, 1989.

[14] M. Verhaegen and V. Verdult. *Filtering and System Identification - A Least Squares Approach*, pages 28–32. Cambridge University Press, 2007.

[15] Rodney C. Wingrove. A study of guidance to reference trajectories for lifting re-entry at supercircular velocity. *NASA Technical report*, 1963.

[16] Rodney C. Wingrove. Survey of atmosphere re-entry guidance and control methods. *American Institute of Aeronautics and Astronautics*, 1(9), 1963.

[17] Curtis Zimmerman, Greg Dukeman, and John Hanson. Automated method to compute orbital reentry trajectories with heating constraints. *Journal of Guidance, Control, and Dynamics*, 26(4), 2003.

[18] Daniel Zwillinger. *Handbook of Differential Equations*. Academic Press, London, 3 edition, 1997.